Journal of Biomedical Optics

SPIEDigitalLibrary.org/jbo

Localized thermal mapping using coherent anti-Stokes Raman spectroscopy

Hope T. Beier
Gary D. Noojin
Benjamin A. Rockwell

SPIE

Localized thermal mapping using coherent anti-Stokes Raman spectroscopy

Hope T. Beier,[a] Gary D. Noojin,[b] and Benjamin A. Rockwell[a]
[a]Air Force Research Laboratory, 4141 Petroleum Road, Building 3260 Fort Sam Houston, Texas 78234
[b]TASC, Inc., 4141 Petroleum Road, Building 3260, Fort Sam Houston, Texas 78234

Abstract. Coherent anti-Stokes Raman scattering (CARS) spectroscopy is explored as a tool for obtaining microscale thermal measurements. A single femtosecond oscillator is used to pump a photonic crystal fiber to provide the broadband Stokes pulse. The CARS signals from the broad OH-stretching modes between 3000 and 3600 cm^{-1} are shown to correlate with temperature with an accuracy of ±1°C for water and ±1.5°C for phosphate-buffered saline. Local variation of temperature is mapped on a microscopic level, using black-dyed microspheres as thermal sources.
[DOI: 10.1117/1.JBO.17.8.080501]

Keywords: coherent anti-Stokes Raman scattering; Raman spectroscopy; multiphoton microscopy; temperature.

Paper 12272L received May 2, 2012; revised manuscript received Jun. 21, 2012; accepted for publication Jun. 21, 2012; published online Jul. 10, 2012.

Temperature measurement at the microscopic level is a valuable tool for studying the thermodynamics of biological systems. Infrared (IR) thermal microscopy has been used to map the local temperature in biological samples; however, this approach is limited by the high IR absorption of water, allowing only the surface temperature to be accurately recorded.[1] The spatial resolution of the IR approach is also on the order of 10 μm, precluding the possibility for localized cellular measurements. Thermal sensitivity of certain fluorescent dyes, such as Rhodamine B, has also been exploited for thermal mapping.[2] However, because this approach typically monitors change in fluorescence intensity, a reference dye with a different temperature dependence is often required to account for variations in excitation intensity. These dyes may also be difficult to introduce intracellularly and may prevent simultaneous monitoring with other fluorescent probes.

Spontaneous Raman scattering has recently been used to monitor temperature in aqueous samples.[3] The hydroxyl-stretching band of water between 3100 and 3700 cm^{-1} demonstrates a dependence on temperature, which enables thermal monitoring in aqueous samples with an accuracy of ~1°C. However, acquisition times of 8 s were reported, limiting the possibility for monitoring rapid changes in temperature or three-dimensional (3-D) mapping. To overcome the long acquisition times inherent to spontaneous Raman, coherent Raman scattering (CRS) techniques have been developed.[4] CRS techniques are nonlinear processes in which the chemical signature of a molecule is probed by simultaneous excitation with two frequencies with a difference, $\omega_{pump} - \omega_{Stokes}$, that matches the vibrational frequency of the molecule. The most common of these techniques, coherent anti-Stokes Raman scattering (CARS), uses spectral filtering to detect the generated anti-Stokes signal, ω_{as}, at $\omega_{as} = 2\omega_{pump} - \omega_{Stokes}$.[4]

In this letter, we used CARS to acquire local temperature directly using the aqueous Raman band, thus removing the necessity for exogenous dyes or mechanical probes. As illustrated in Fig. 1, a single femtosecond oscillator (760 nm, 130 fs, 80 MHz, 3 W) pumps a photonic crystal fiber (NKT Photonics, Femtowhite) with 250 mW average power to generate a supercontinuum with 40% coupling efficiency. After filtering, this broadband Stokes beam spans from 850 to 1070 nm, allowing for simultaneous acquisition of all Raman frequencies of interest. The pump and Stokes beams are recombined with a 750-nm band pass filter and routed into a customized scanning microscope (40×, water 1.0 NA). A motorized stage in the pump path is used to fine-tune the temporal overlap between the two beams. The CARS signals are collected in transmission by a second objective lens (60×, oil 1.2 NA) and directed into a spectrograph fitted with a CCD camera (Andor, iDus). Typical measured powers at the sample were ~10 mW of pump and ~5 mW of supercontinuum; spectra were collected with an acquisition time of 10 ms.

As demonstrated in Fig. 2(a), there is a variation in the relative amplitude of the two Gaussian components of the water hydroxyl-stretching modes with temperature. It is theorized that the coupling of hydrogen bonds to the hydroxyl group reduces the energy (wavenumber) of the hydroxyl-stretching. With increasing temperature, hydrogen bonding decreases, shifting the relative intensity of peaks toward the higher frequency mode.[5] As demonstrated in Fig. 2(b), to measure the relative intensity in each mode, the OH-stretching modes were fit individually to two Gaussian profiles with peak centers held to 3260 and 3424 cm^{-1}. Before fitting, the spectra were normalized to the isosbestic point, observed at 3295 cm^{-1}, to account for the slight changes in coupling efficiency into the spectrograph as a result of temperature variation. These changes were found to affect only the overall intensity of the spectra, not the peak ratios. The isosbestic point is at a lower frequency than the ~3400 cm^{-1} for spontaneous Raman, as is expected due to red-shifting of the CARS spectrum from nonresonant background contributions.[6]

To determine the accuracy of using the CARS signal to measure temperature, various temperatures of water and phosphate buffered saline (PBS), heated in a water bath, were pumped into the sample dish. A thermistor was placed at the edge of the field view to measure the local temperature near the focal volume. In Fig. 3, the ratio of the areas of the lower-frequency CARS peak (peak 1) to higher-frequency peak (peak 2) is shown as a function of local temperature, in water (a) and PBS (b), as measured by the thermistor. Each point is the average of five to 10 spectra for each 0.1°C, taken throughout three separate runs. The ratio of the areas provides a reasonable cubic fit to the temperature. The accuracy of this approach was determined by randomly

Address all correspondence to: Hope T. Beier, Air Force Research Laboratory, 4141 Petroleum Road, Building 3260, Fort Sam Houston, Texas 78234. Tel: 210-539-8199; E-mail: hopebeier@gmail.com

0091-3286/2012/$25.00 © 2012 SPIE

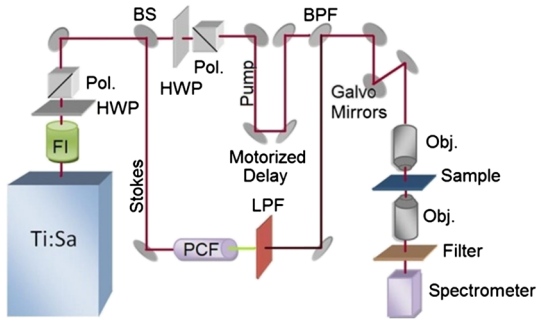

Fig. 1 Diagram of our CARS setup. FI is a Faraday isolator, HWP are achromatic half waveplates, Pol. are Glan-laser polarizers, BS is a plate beam splitter, and PCF is the photonic crystal fiber.

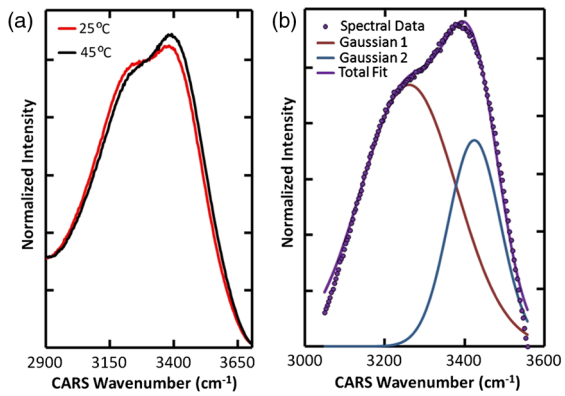

Fig. 2 (a) CARS spectra of water at 25°C and 45°C, demonstrating the dependence of the OH-stretching modes on temperature. (b) CARS spectra fitted to two Gaussian profiles to determine the area of each peak.

selecting approximately 10% of the individual spectra as a validation set and calculating the residuals between the predicted and measured temperatures. These results are shown in the insets of Fig. 3. Accuracy of the data was found to be ±1°C for water and ±1.5°C for PBS. For comparison, partial least squares and principle component regression were also performed on the same data sets; these methods resulted in validation accuracy similar to that of the Gaussian fits. In addition to its temperature dependence, the hydrogen bond strength is also affected by the local ionic composition and concentration. In these measurements, the predicted temperature between deionized water and PBS was found to vary by as much as 4°C at lower temperatures. Thus, these measurements are appropriate for systems containing relatively homogeneous ionic distributions.

With near infrared (NIR) excitation, we should also take heating of the sample volume into consideration. The temperature increase for highly focused excitation beams with average power of 100 mW and $\lambda < 1070$ nm has been found to be less than 3°C, and less than 0.25°C for 850-nm excitation.[7] Given our lower average power of 15 mW and that two-thirds of our excitation power was centered at 760 nm, where water absorption is low, the temperature in our excitation volume should not have increased by more than 0.2°C during the measurement.

To demonstrate the thermal mapping capabilities of this approach, 1-μm-diameter black-dyed polystyrene microspheres were used as local thermal sources, due to their absorbance of

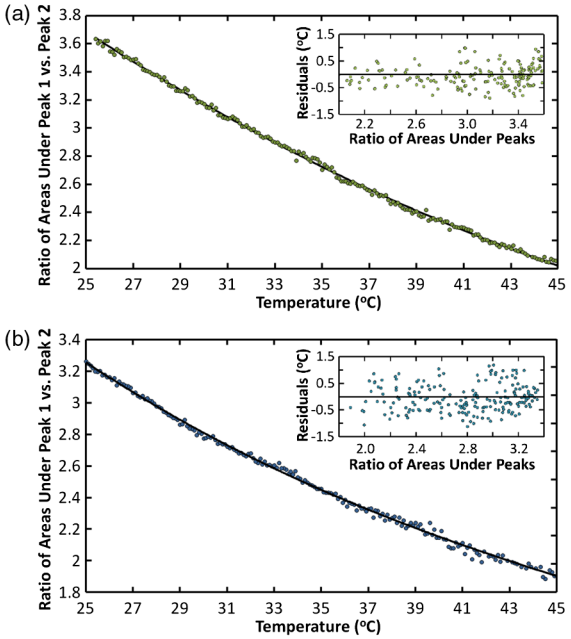

Fig. 3 Ratio of the areas of Peak 1 to Peak 2 of the CARS OH-stretching bands as a function of temperature between 25°C and 45°C in DI water (a) and PBS (b). Insets in each figure are the residuals between the predicted and measured temperatures for the validation set.

NIR excitation light. The focal volume, at a height of 1.5 μm above the plane of the microspheres, was scanned parallel to the spectrograph slit using a galvanometer mirror. Motorized stage scanning provided the x-direction scan. A thermal map over several individual and small clusters of these microspheres is shown in Fig. 4.

To gauge the accuracy of this thermal map, the expected temperature rise is determined using the standard heat-diffusion equation:

$$C\rho\frac{\partial T}{\partial t} = k\frac{1}{r^2}\frac{\partial}{\partial r}\left(r^2\frac{\partial T}{\partial r}\right) + q(r), \tag{1}$$

where k is the thermal conductivity, C is the specific heat, and ρ is the density. The heat source, $q(r)$, is defined as $q = \sigma_{\text{abs}} I(t)/V$, where σ_{abs} is the absorption cross-section, $I(t)$ is the irradiance of the laser source, and V is the volume of the microsphere.[8] The thermal time constant, $\tau_c = \omega_o^2/(4\kappa_w)$, a measure of how quickly steady state is

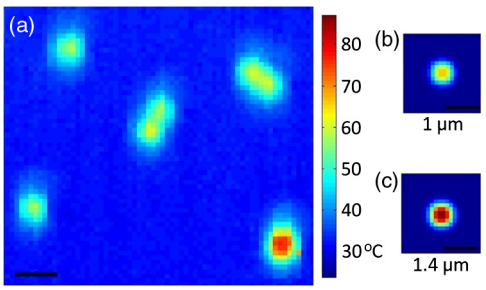

Fig. 4 (a) Map of the temperature 1.5 μm above 1 μm microspheres, used as local absorbers. The temperature at the microsphere surface for our experimental irradiance is modelled for 1 μm (b) and 1.4 μm (c) microspheres. The scale bar is 2 μm.

reached, is approximately 500 ns in our case, given ω_o as the Gaussian beam radius and κ_w, the thermal diffusivity of water (1.43×10^{-7} m^2 s^{-1}).[9] Because this value is much larger than the interpulse interval (12 ns) and our acquisition time is much longer (10 ms), we assume that the heating can be treated as quasi-CW and that a steady state is reached within the measurement interval and thus, we can neglect the temporal derivative. The two reduced differential equations, one for the microsphere that contains the heat source and one for the surrounding fluid with no heat source, can be solved using boundary conditions that assume that the temperature and $k\frac{\partial T}{\partial r}$ are continuous at the microsphere surface, where $r = R$, and that $T \rightarrow$ ambient as $r \rightarrow \infty$. We obtain a value for the temperature, T_s at the surface of the microsphere:

$$T_s = \frac{\sigma_{abs} I}{4\pi R k_f}, \tag{2}$$

and a thermal profile in the surrounding fluid, $T(r) = T_s(R/r)$.

Using a reported value for the absorption cross-section ($1.37\text{E}-10$ cm^2/particle, no λ specified[10]) and applying the Gaussian beam approximation to determine the irradiance of our beam at the plane of the microspheres, we can model the local temperature rise near the microsphere surface. Figure 4(b) shows the thermal profile surrounding a 1-μm-diameter black-dyed microsphere. This model slightly overestimates the temperature rise compared to the experimental results, which is possibly a result of overestimation of the absorption cross-section. The temperature rise in the model is also more confined in proximity to the microsphere; this result was expected since the model did not account for convection of the heat from the microsphere surface that is present in the real system. However, these results suggest that we have successfully mapped the local temperature around the microspheres. One microsphere appears significantly hotter than the other individual particles. This increase can be explained as an abnormally large microsphere in the polydisperse batch, as modeled in Fig. 4(c).

We have demonstrated a method of remotely acquiring the local temperature of aqueous samples without the introduction of dyes of other materials into the sample. Our approach uses a single femtosecond oscillator with a photonic crystal fiber to extend the spectral bandwidth and is a relatively inexpensive addition to an existing multi-photon microscope. As a multiphoton approach, a map of the local temperature was provided with diffraction-limited spatial resolution (<1 μm). Total power delivered to sample is 15 mW with an integration time of 10 ms, a significant improvement of the previously demonstrated spontaneous Raman approach that required 70 mW of power at the sample with an integration time of 8 s.[3] Acquisition time may be decreased further with a more sensitive camera (e.g., EM-CCD) or with dual photomultiplier tube or avalanche photodiode detectors with proper spectral filtering.

Acknowledgments

This research was performed while Hope Beier held an Air Force Office of Scientific Research (AFOSR) sponsored National Research Council Research Associateship Award at the Air Force Research Laboratory/Human Performance Wing and AFOSR LRIR Award #12RH01COR. Contract support was provided under AFRL contract number FA8650-08-D-6930.

References

1. B. Kateb et al., "Infrared thermal imaging: a review of the literature and case report," *Neuro. Image* **47**(Suppl. 2), T154–T162 (2009).
2. J. Sakakibar and R. J. Adrian, "Whole field measurement of temperature in water using two-color laser induced fluorescence," *Exp. Fluids* **26**(1–2), 7–15 (1999).
3. V. Pikov and P. H. Siegel, "Thermal monitoring: Raman spectrometer system for remote measurement of cellular temperature on a microscopic scale," *IEEE Eng. Med. Biol. Mag.* **29**(1), 63–71 (2010).
4. A. Zumbusch, G. R. Holtom, and X. S. Xie, "Three-dimensional vibration imaging by coherent anti-Stokes Raman scattering," *Phys. Rev. Lett.* **82**(20), 4142–4145 (1999).
5. G. E. Walrafen et al., "Temperature-dependence of the low-frequency and high-frequency Raman-scattering from liquid water," *J. Chem. Phys.* **85**(12), 6970–6982 (1986).
6. G. E. Walrafen, M. S. Hokmabadi, and W. H. Yang, "Raman isosbestic points from liquid water," *J. Chem. Phys.* **85**(12), 6964–6969 (1986).
7. A. Schonle and S. Hell, "Heating by absorption in the focus of an objective lens," *Opt. Lett.* **23**(5), 325–327 (1998).
8. M. I. Tribelsky et al., "Laser pulse heating of spherical metal particles," *Phys. Rev. X* **1**(2), 021024 (2011).
9. W. Denk, D. W. Piston, and W. W. Webb, Multi-Photon Molecular Excitation in Laser-Scanning Microscopy, Chapter 28, in Handbook of Biological Confocal Microscopy, J. B. Pawley, Ed., pp. 535–549,Springer Science+Business Media, New York, NY (2006).
10. Y.-K. Jeong and J. Lee, "Optical properties of polystyrene black dyed microspheres," *Curr. Appl. Phys.* (2012) (in press).